VIBRATION CONTROL IN A PITCH-PLANE SUSPENSION MODEL WITH MR SHOCK ABSORBERS

BOGDAN SAPIŃSKI
PAWEŁ MARTYNOWICZ

Department of Process Control, University of Science and Technology, Cracow
e-mail: deep@agh.edu.pl; pmartyn@agh.edu.pl

The paper is concerned with the experimental study of vibration control in a suspension equipped with independently controlled magnetorheological shock absorbers (MRAs) in front and rear sections. For research purposes, the pitch-plane suspension model with bounce and pitch motions was considered. This suspension model was tested in open-loop and feedback system configurations under harmonic and square excitations. The experiments were conducted on a specially designed experimental setup with a data acquisition and control system configured in the MATLAB/Simulink environment. The obtained results reveal effectiveness of MRAs for vibration suppression in the investigated suspension model.

Key words: MR shock absorber, pitch-plane suspension model, LQ control

1. Introduction

Typical vehicle suspension systems with passive shock absorbers are characterised with unavoidable compromise between road roughness attenuation and drive stability of the vehicle. That is why active and semi-active vehicle suspensions are used. In semi-active suspensions, conventional springs are retained but passive shock absorbers are replaced with controllable shock absorbers (Nagai *et al.* 1996). Vibro-isolation properties of semi-active suspensions are close to those of active ones. Semi-active suspension systems use external power only to adjust damping levels and operate the controller and set of sensors, whereas active systems require significant amount of external energy to power the actuators. An example of semi-active suspension is the

Magnetic Ride Control system that has been used in Cadillac Seville STS cars since 2002. This system is equipped with MRAs made by Delphi Automotive Systems (MagneRide). Similar shock-absorbers are used in suspensions of Corvette racing cars. Such systems are durable and give very wide capabilities of adaptation to drive conditions and enhance vehicle-manoeuvring possibilities.

The application of MRAs was successfully investigated in vibration control of car systems (mainly concerning a quarter car) among others by (Pare, 1998; Song, 1998; McLellan, 1998; Kiduck and Doyoung, 1999; Simon, 2000) and others from a research group at Virginia Tech (Virginia Tech, 2002). Results of computer simulations for such a scaled quarter car model provided in among others (Virginia Tech, 2002; Yao *et al.*, 2002) revealed that with semi-active damping control vibration of the suspension system is well controlled. The group from Virginia Tech evaluated the performance of MR suspensions for a quarter car model test facility and for a heavy truck on a road under control schemes of skyhook, groundhook and hybrid semi-active control. That was also partially confirmed in the initial phase of experimental research described in (Sapiński *et al.*, 2003).

The suspension model selected for the purpose of vibration analysis is largely dependent on the objective of the analysis. The review of simple and credible models that can be useful for fundamental vibration analysis in terms of resonant frequencies and forced vibration responses of sprung and unsprung masses provided in (Ahmed, 2002) shows that the vibration response of vehicles to different excitations can be investigated through analysis of various in-plane models.

Because the wheelbase of the majority of ground vehicles is significantly larger than the track width, roll motions can be considered negligible compared to magnitudes of vertical and pitch motions. That is why we focused on a two degree-of-freedom (2 DOF) pitch-plane model of a suspension equipped with MRAs (Martynowicz, 2003). This model enables us to study qualitative bounce and pitch motions of the sprung mass, assuming negligible contributions due to axle and tire assembly. In this case, the road input is taken to be the same as the wheels and is suitable for the estimation of bounce and pitch resonance frequencies. This model is also considered applicable for study of off-road vehicles without the sprung suspension, where the stiffness and damping elements relate to the properties of tires alone.

The paper reports an experimental study of vibration control in a semi-active suspension equipped with MRAs. For this purpose, we built an experimental setup of the 2 DOF pitch-plane suspension model. We employed MRAs of the RD-1005-3 series made by Lord Corporation (http://www.lord.com).

For the purpose of controller design, real-time data acquisition and control, MATLAB/Simulink environment was employed (The Mathworks, 2003). In the control system, we used solution to a linear-quadratic (LQ) problem formulated for this part of the system which does not contain MRAs and the hysteresis inverse model of the MRA (Sapiński and Martynowicz, 2004).

2. Pitch-plane suspension model

For the purpose of the suspension analysis, we introduce a 2 DOF pitch-plane model. Using this type of model, we can analyse pitch and vertical motions of the suspended body, which prove to be the most inconvenient (the lowest threshold of toleration) for a human body. This type of model is an introduction to analysis of the whole-vehicle behaviour.

The model of suspension to be considered is shown in Fig. 1. The vehicle body is simulated by a rigid rectangle-intersection beam of mass m, moment of inertia I, total length L, width a, height b and centre of gravity (c.o.g.) in P_g. The beam is supported in points P_f and P_r by two identical spring-MRA sets (hereinafter called suspension-sets), which are subject to bottom kinematic displacement excitations similar to these acting upon a conventional vehicle suspension. The distances from P_g to P_f and from P_g to P_r are denoted by l_f and l_r (respectively). The presented model possesses two degrees of freedom, which can be described as the vertical (bounce) displacement x and pitch displacement φ of the c.o.g. (Ahmed, 2002; Fuller, 1996; Sapiński and Martynowicz, 2004).
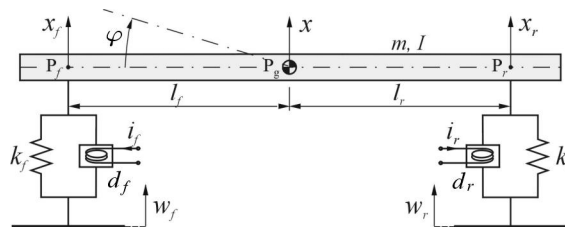

Fig. 1. 2 DOF pitch-plane suspension model

Excitations applied to the bottom of the front and rear suspension-sets are denoted by w_f and w_r, respectively, displacements of points P_f and P_r – by x_f and x_r, resultant forces exerted on the front and rear suspension-sets –

by F_f and F_r (respectively). Assuming a vehicle with a long base $(l_f + l_r)$, therefore $\sin\varphi \cong \varphi$, yields

$$x_f = x + l_f\varphi \qquad\qquad x_r = x - l_r\varphi \qquad\qquad (2.1)$$

Let us introduce formulas describing forces F_f and F_r

$$F_f = F_{S,f} + F_{MR,f} \qquad\qquad F_r = F_{S,r} + F_{MR,r} \qquad\qquad (2.2)$$

where $F_{S,f}$ and $F_{S,r}$ are respective spring forces

$$F_{S,f} = -k_{S,f}(x_f - w_f) \qquad\qquad F_{S,r} = -k_{S,r}(x_r - w_r) \qquad\qquad (2.3)$$

Designations $F_{MR,f}$, $F_{MR,r}$ represent resistance forces of MRAs denoted by d_f and d_r, respectively. To obtain the formula for $F_{MR,f}$, a Spencer model of the MRA is invoked (Fig. 2), governed by the system of equations

$$\dot{z}_f = -\gamma|(\dot{x}_f - \dot{w}_f - \dot{y}_f)z_f|z_f - \beta(\dot{x}_f - \dot{w}_f - \dot{y}_f)|z_f|^2 + A(\dot{x}_f - \dot{w}_f - \dot{y}_f)$$

$$\dot{y}_f = \frac{1}{c_0 + c_1}[\alpha z_f + c_0(\dot{x}_f - \dot{w}_f) + k_0(x_f - w_f - y_f)] \qquad\qquad (2.4)$$

$$F_{MR,f} = -c_1\dot{y}_f - k_1(x_1 - x_0)$$

where parameters: α, β, γ, A, c_0, c_1, k_0, k_1, x_0 describe non-linear relationships which are inherent features of the MRA (Spencer, 1996). These parameters (varying with piston velocity of the MRA) are presented in Table 1 and Table 2 (Sapiński, 2004) in function of frequency and amplitude of the sine excitation. The equations modeling rear MRA behaviour and force $F_{MR,r}$ can be defined in an analogous manner.
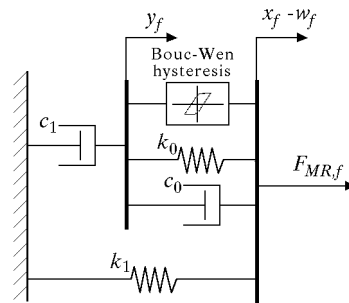

Fig. 2. MRA model by Spencer

Table 1. Parameters of Spencer's model: frequency $1\,\text{Hz}$, amplitude $20 \cdot 10^{-3}\,\text{m}$ (peak to peak)

Current	Parameter value								
I	α	c_0	c_1	k_0	A	$\beta \cdot 10^4$	$\gamma \cdot 10^4$	k_1	$x_0 \cdot 10^{-2}$
[A]	[N/m]	[Ns/m]	[Ns/m]	[N/m]	[–]	[1/m^2]	[1/m^2]	[N/m]	[m]
0.0	29879.5	348.6	69870	1181.6	17.664	348.217	394.71	705.8	25.135
0.2	49069.8	1138.9	33713	1807.1	31.684	42.071	221.31	550.8	31.466
0.4	52501.5	2138.8	38551	674.2	36.483	14.834	42.21	633.0	27.011

Table 2. Parameters of Spencer's model: frequency $4\,\text{Hz}$, amplitude $3 \cdot 10^{-3}\,\text{m}$ (peak to peak)

Current	Parameter value								
I	α	c_0	c_1	k_0	A	$\beta \cdot 10^4$	$\gamma \cdot 10^4$	k_1	$x_0 \cdot 10^{-2}$
[A]	[N/m]	[Ns/m]	[Ns/m]	[N/m]	[–]	[1/m^2]	[1/m^2]	[N/m]	[m]
0.0	70082.3	1013.6	12414	2973.4	4.042	226.307	571.24	835.4	24.242
0.2	76315.9	1838.6	48180	2922.8	14.803	2.728	305.84	839.0	23.561
0.4	86070.1	4010.5	50239	2903.4	17.146	1.317	99.03	695.9	26.891

In the analysed system, we consider the initial deflection of springs and MRAs due to the suspended load (the beam) as a zero initial condition of displacements x and φ. This enables us to neglect the gravity forces of the sprung mass and to describe the dynamics of the $2\,\text{DOF}$ pitch-plane suspension model by expressions (2.5). Equations (2.5) present balances of forces and moments of forces

$$m\ddot{x} = F_f + F_r \qquad\qquad I\ddot{\varphi} = F_f l_f - F_r l_r \tag{2.5}$$

3. Experimental setup

For the purpose of the $2\,\text{DOF}$ pitch-plane suspension analysis, an experimental setup was devised comprising data acquisition and control equipment connected to PC-based communication and control software.

As our analysis is limited to pitch-plane oscillations, the experimental setup should conform to appropriate construction demands, namely transverse rigidity. All motion components orthogonal to the pitch-plane or other than pitch and bounce should be eliminated. This implies introduction of appropriate central guiding elements with adequately small friction forces. All joints should have a high transverse rigidity.

Another demand is the excitations are stationarity. A limited output of the excitation sources available in laboratory conditions implies constraints to the total mass and moment of inertia of the sprung system.

The experimental set-up (Fig. 3) consists of: steel beam with rectangular intersection (1) as a load element (vehicle body), two identical suspension-sets: spring (2) – MRA (3), central roller guiding (4) and two kinematic excitation sources. Each suspension-set is built as a parallel connection of a vertically mounted MRA inside and an outer screw-cylindrical reflex spring guided onto two thin-wall sleeves (5). The sleeves are guided one inside the other with a teflon slide ring between them. Both sleeves possess outer flanges as the spring support. Each suspension-set is connected at the top with the beam and at the bottom with the shaker by means of pin joints.
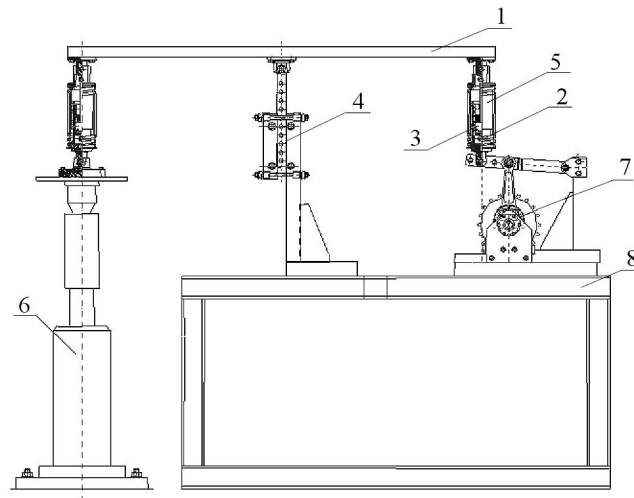

Fig. 3. Experimental setup

Two types of kinematic shakers were available in the experiments. One of them was an electro-hydraulic cylinder (6) with the maximum force output $2.5 \cdot 10^3$ N and maximum stroke $50 \cdot 10^{-3}$ m. It was anchored to the foundation with bolts. The other shaker was a $3.5 \cdot 10^3$ W asynchronous electric motor with a circular cam crank mechanism (7). The motor was supplied by an electronic inverter enabling smooth control of rotation speed and excitation frequency in the range of (3.5,10) Hz. The beam's c.o.g. was connected to the vertical guiding rail (4) by means of a roller bearing guaranteeing longitudinal and transversal rigidity of the system. Guiding bar (4) and shaker (7) were both mounted on the rigid cubicoid frame (welded section steel) (8).

Numerical values of parameters describing the mechanical elements are presented in the Table 3.

Table 3. Technical specifications data

Parameter	Designation	Value
Distance (P_g, P_f)	l_f [m]	0.7
Distance (P_g, P_r)	l_r [m]	0.7
Total length of the beam	L [m]	1.5
Width of the beam	a [m]	0.124
Height of the beam	b [m]	0.173
Mass of the beam	m [kg]	253.3
Moment of inertia of the beam	I [kg m^2]	49.20
Elasticity factor of the front (rear spring)	$k_{S,f}$ ($k_{S,r}$) [N/m]	42016
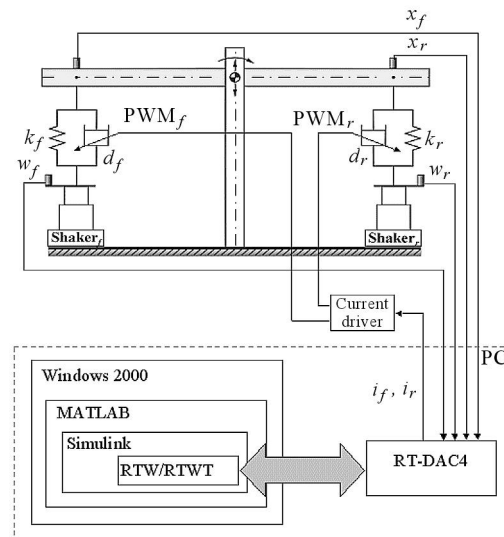
Fig. 4. Diagram of data acquisition and control system

All measurements were conducted by means of four PSz-20 transducers (two of them located on the beam – x_f and x_r, and the other two on the shakers – w_f and w_r) and a multipurpose I/O board of the RT-DAC4 series placed in a standard PC (Fig. 4). The MATLAB/Simulink environment with RTWT (Real-Time Windows Target) extension of RTW (Real-Time Workshop) toolbox (The Math Works, 2003) running on the Windows 2000 operating system

completed the set-up. On the basis of x_f and x_r measurements, the vertical displacement x and pitch displacement φ of the beam's c.o.g. were received. MRAs currents i_f, i_r calculated in the MATLAB/Simulink were output by means of RTWT/RTW and RT-DAC4, and then converted to PWM signals.

4.   Experiments

In the next subsections, we present scenario and results of the experiments conducted in open-loop and feedback system configurations with the help of the experimental setup introduced above.

4.1.   Open-loop system

To analyse the open-loop 2 DOF pitch-plane system, we observed the centre of gravity P_g bounce and pitch responses (i.e. x and φ) to bottom excitations applied to the front suspension-set. One-side (front or rear) excitation is a typical situation during driving the vehicle. Values of x and φ can be calculated as follows

$$x = \frac{x_f + x_r}{2} \qquad\qquad \varphi = \frac{x_f - x_r}{l_f + l_r} \tag{4.1}$$

We considered two cases of the passive suspension (open-loop) system: in the first case (hereinafter called OS1) we supplied the coils of both MRAs with no current, in the second case (hereinafter called OS2) – with the current 0.1 A.

Let us introduce quality indexes to measure root-mean-square (RMS) accelerations of beam bounce $(4.2)_1$ and pitch $(4.2)_2$, and shaker $(4.2)_3$ motions in the time range of $(0, t_{fin})$

$$RMS_{\ddot{x}} = \sqrt{\int_0^{t_{fin}} [\ddot{x}(t)]^2 \, dt} \qquad\qquad RMS_{\ddot{\varphi}} = \sqrt{\int_0^{t_{fin}} [\ddot{\varphi}(t)]^2 \, dt}$$

$$RMS_{\ddot{w}_f} = \sqrt{\int_0^{t_{fin}} [\ddot{w}_f(t)]^2 \, dt} \tag{4.2}$$

To obtain RMS acceleration transmissibilites $T_{\ddot{x}}$ $(4.3)_1$ and $T_{\ddot{\varphi}}$ $(4.3)_2$, we measured the system response to front sine excitation series in the range of

$(1,10)$ Hz, and then calculated $RMS_{\ddot{x}}$, $RMS_{\ddot{\varphi}}$ and $RMS_{\ddot{w}_f}$ indexes for all analysed frequencies

$$T_{\ddot{x}} = \frac{RMS_{\ddot{x}}}{RMS_{\ddot{w}_f}} \qquad\qquad T_{\ddot{\varphi}} = \frac{l_f RMS_{\ddot{\varphi}}}{RMS_{\ddot{w}_f}} \qquad\qquad (4.3)$$

The results are presented in Fig. 5 and Fig. 6. On the basis of these measurements, we calculated the frequency f-weighted RMS bounce acceleration transmissibility index T_W (4.4), according to the weighting factors $W(f)$ as in ISO 2631-1 (1997) – see Table 4 in Subsection 4.2

$$T_W = \sqrt{\sum_f [W(f)T_{\ddot{x}}(f)]^2} \qquad\qquad (4.4)$$
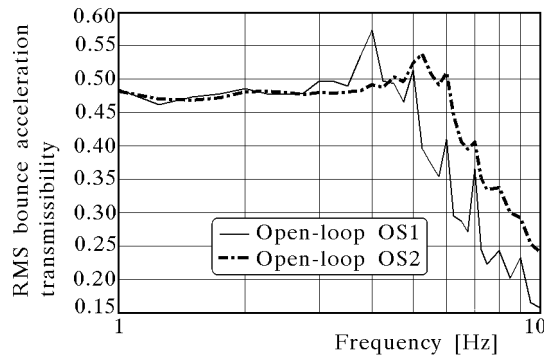
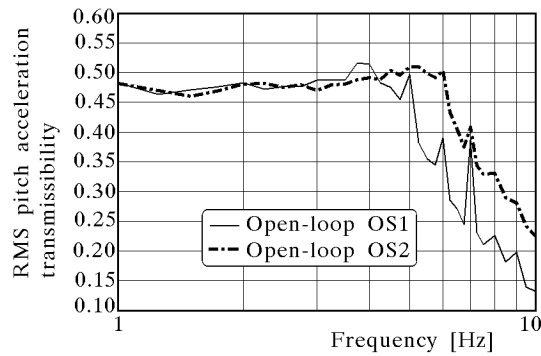Fig. 5. RMS bounce acceleration transmissibility

Fig. 6. RMS pitch acceleration transmissibility

Besides the resonance frequencies of OS1 are: $f_x \approx 3.1$ Hz (bounce), $f_\varphi \approx 5.0$ Hz (pitch), the internal coupling between the two modes causes

the shift of the transmissibilities' maximums for one-side excitations. Both characteristics reveal some embedded features of the experimental setup: at certain frequencies we observe high acceleration peaks. That means that at these frequencies there is an increased damping and rigidity of the analysed suspension-set due to the MRA nonlinearity.

In further analysis, we assume that the front and rear suspension-sets are identical, i.e. possessing equal stiffness factors of the front and rear springs ($k_{S,f} = k_{S,r} = k$) and equal for both MRAs values of parameters: α, β, γ, A, c_0, c_1, k_0, k_1, x_0.

4.2. Feedback system

As stated in the beginning of the study, one of the basic suspension purposes is the optimisation of drive comfort, thus minimisation of vibrations affecting humans (Kowal, 1996). Accordingly, we introduce a feedback system whose aim is to reduce RMS bounce and pitch acceleration transmissibility indexes $T_{\ddot{x}}$, $T_{\ddot{\varphi}}$ and the frequency weighted RMS bounce acceleration transmissibility index T_W using the weighting factors as in ISO 2631-1 (1997). To accomplish it, we construct a semi-active cascade control system consisting of two stages (see Fig. 7). In the first stage, the system determines values of forces $F^*_{MR,f}$, $F^*_{MR,r}$, which minimise the assumed quality index J (4.5)$_1$, where: $q_{\ddot{x}}$, $q_{\ddot{\varphi}}$ are weighting factors of $\ddot{x}$ and $\ddot{\varphi}$, respectively (J depends on transmissibility squares and $RMS_{\ddot{w}_f}$ – constant for the chosen excitation type, see equation (4.5)$_2$). In the second stage, the system calculates values of currents i_f, i_r, which cause MRAs to produce resistance forces $F_{MR,f}$, $F_{MR,r}$ as close to $F^*_{MR,f}$, $F^*_{MR,r}$ as possible to produce for instantaneous relative velocities of beam and shakers

$$J = \int_0^{t_{fin}} \left\{ q_{\ddot{x}}[\ddot{x}(t)]^2 + q_{\ddot{\varphi}}[\ddot{\varphi}(t)]^2 \right\} dt \qquad J = \left(q_{\ddot{x}} T_{\ddot{x}}^2 + \frac{q_{\ddot{\varphi}} T_{\ddot{\varphi}}^2}{l_f^2} \right) RMS_{\ddot{w}_f} \quad (4.5)$$
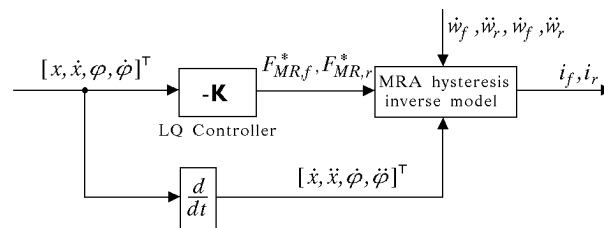

Fig. 7. Controller diagram

The first stage of the control task utilises the optimal linear-quadratic (LQ) controller – a stabilising controller to be applied in linear dynamic systems (Mitkowski, 1991). The LQ control is the optimal control with respect to the assumed quadratic quality index J_{LQ} (4.9), similar to J (4.5)$_1$. In order that the linearity assumption and task conditions (minimised accelerations) be fulfilled, the model governed by equations (2.4)-(2.5) was modified accordingly, yielding a matrix state space equation, see (4.6), in which the state vector $\boldsymbol{X}$, Eq (4.7)$_1$, now includes velocities $\dot{x}$ and $\dot{\varphi}$ as well. Forces $F_{MR,f}$ and $F_{MR,r}$ (produced by MRAs d_f and d_r) defined by nonlinear relationships are transferred to the control vector $\boldsymbol{U}$. In order that the model can be written in a form of a linear state space equation, the control $\boldsymbol{U}$ should incorporate excitations w_f, w_r (4.7)$_2$

$$\dot{\boldsymbol{X}} = \mathbf{A}\boldsymbol{X} + \mathbf{B}U \tag{4.6}$$

where

$$\boldsymbol{X} = [x, \dot{x}, \varphi, \dot{\varphi}]^\top \qquad\qquad \boldsymbol{U} = [F_{MR,f}, F_{MR,r}, w_f, w_r]^\top \tag{4.7}$$

$$
\mathbf{A} = \begin{bmatrix}
0 & 1 & 0 & 0 \\
-\dfrac{2k}{m} & 0 & -\dfrac{k(l_f - l_r)}{m} & 0 \\
0 & 0 & 0 & 1 \\
-\dfrac{k(l_f - l_r)}{I} & 0 & -\dfrac{k(l_f^2 + l_r^2)}{I} & 0
\end{bmatrix}
\qquad
\mathbf{B} = \begin{bmatrix}
0 & 0 & 0 & 0 \\
\dfrac{1}{m} & \dfrac{1}{m} & \dfrac{k}{m} & \dfrac{k}{m} \\
0 & 0 & 0 & 0 \\
\dfrac{l_f}{I} & -\dfrac{l_r}{I} & \dfrac{kl_f}{I} & -\dfrac{kl_r}{I}
\end{bmatrix}
$$
$$\tag{4.8}$$

The pair $(\mathbf{A}, \mathbf{B})$ is stabilisable, hence the first necessary and sufficient condition for precisely one optimal control strategy is fulfilled (Mitkowski, 1999). Invoking (4.7), the quality index in the LQ problem for the time horizon $(0, t_{fin})$ is written in the form

$$
\begin{aligned}
J_{LQ} = \int_0^{t_{fin}} &\Big\{ q_x [x(t)]^2 + q_\varphi [\varphi(t)]^2 + q_{\dot{x}} [\dot{x}(t)]^2 + q_{\dot{\varphi}} [\dot{\varphi}(t)]^2 + q_{\ddot{x}} [\ddot{x}(t)]^2 + \\
&+ q_{\ddot{\varphi}} [\ddot{\varphi}(t)]^2 + r_{F_{MR,f}} [F_{MR,f}(t)]^2 + r_{F_{MR,r}} [F_{MR,r}(t)]^2 + \\
&+ r_{w_f} [w_f(t)]^2 + r_{w_r} [w_r(t)]^2 + 2 r_{w_f w_r} w_f(t) w_r(t) \Big\} \, dt
\end{aligned}
\tag{4.9}
$$

where $\ddot{x}(t)$ and $\ddot{\varphi}(t)$ are taken from the left-hand side of (4.6). After this substitution, we can write the quality index according to the LQ definition

$$
J_{LQ} = \int_0^{t_{fin}} \Big\{ [\boldsymbol{X}(t)]^\top \mathbf{Q} \boldsymbol{X}(t) + [\boldsymbol{U}(t)]^\top \mathbf{R} \boldsymbol{U}(t) + 2 [\boldsymbol{X}(t)]^\top \mathbf{N} \boldsymbol{U}(t) \Big\} \, dt
\tag{4.10}
$$

where $\mathbf{Q}$, $\mathbf{R}$, $\mathbf{N}$ are described as follows

$$
\mathbf{Q} = \begin{bmatrix} q_x + \dfrac{4k^2}{m^2}q_{\ddot{x}} & 0 & 0 & 0 \\ 0 & q_{\dot{x}} & 0 & 0 \\ 0 & 0 & q_\varphi + \dfrac{4k^2 l^4}{I^2}q_{\ddot{\varphi}} & 0 \\ 0 & 0 & 0 & q_{\dot{\varphi}} \end{bmatrix}
$$

$$
\mathbf{R} = \begin{bmatrix} r_{F_{MR,f}} + a_1 & a_2 & ka_1 & ka_2 \\ a_2 & r_{F_{MR,r}} + a_1 & ka_2 & ka_1 \\ ka_1 & ka_2 & r_{w_f} & r_{w_f w_r} \\ ka_2 & ka_1 & r_{w_f w_r} & r_{w_r} \end{bmatrix}
$$

$$
a_1 = \frac{1}{m^2}q_{\ddot{x}} + \frac{l^2}{I^2}q_{\ddot{\varphi}} \qquad\qquad a_2 = \frac{1}{m^2}q_{\ddot{x}} + \frac{l^2}{I^2}q_{\ddot{\varphi}}
$$

$$
\mathbf{N} = \begin{bmatrix} \dfrac{-2k}{m^2}q_{\ddot{x}} & \dfrac{-2k}{m^2}q_{\ddot{x}} & \dfrac{-2k^2}{m^2}q_{\ddot{x}} & \dfrac{-2k^2}{m^2}q_{\ddot{x}} \\ 0 & 0 & 0 & 0 \\ \dfrac{-2kl^3}{I^2}q_{\ddot{\varphi}} & \dfrac{2kl^3}{I^2}q_{\ddot{\varphi}} & \dfrac{-2k^2 l^3}{I^2}q_{\ddot{\varphi}} & \dfrac{2k^2 l^3}{I^2}q_{\ddot{\varphi}} \\ 0 & 0 & 0 & 0 \end{bmatrix}
$$

(4.11)

where $l_f = l_r = l$ (full symmetry of the 2 DOF pitch-plane suspension system).

The selection of the matrix elements $\mathbf{Q}$, $\mathbf{R}$ was based on the principle that the cost of any variable must be inversely proportional to the squared allowable deflection from the nominal value (Brzzka, 2004). Besides, in order that quality index (4.9) approaches assumed form $(4.5)_1$, the weighting factors of the beam c.o.g. accelerations should be several orders of magnitude larger than the weighting factors of displacements q_x, q_φ, velocities $q_{\dot{x}}$, $q_{\dot{\varphi}}$ and maximal forces $r_{F_{MR,f}}$, $r_{F_{MR,r}}$. On account of the fact that the excitations present in the considered LQ problem are disturbances (they are not subject to control), strong constraints are imposed on w_f and w_r: $r_{w_f} = r_{w_r} = 10^{11}$, $r_{w_f w_r} = 10^{10}$ and these components of the quality index are not taken into account in the evaluation of system behaviour and ride comfort. The weightings of the bounce and pitch displacements are taken as $q_x = q_\varphi = 1$. Additionally, it is assumed that: $r_{F_{MR,f}} = r_{F_{MR,r}} = 16 \cdot 10^{-4}$ (weak constraints upon the maximum values of $F_{MR,f}$ and $F_{MR,r}$ due to reasonable MRA force output margins) and $q_{\ddot{x}} = q_{\ddot{\varphi}} = 10^5$ (large weightings of acceleration in the quality index). To enhance the system behaviour at lower frequencies, we further

assume that $q_{\dot{x}} = q_{\dot{\varphi}} = 10^3$. Such weighting factor values guarantee that all necessary and sufficient conditions for just one optimal control strategy $\boldsymbol{U}^*$ be fulfilled ($\boldsymbol{Q} = \boldsymbol{Q}^\top \geqslant \boldsymbol{0}$, $\boldsymbol{R} = \boldsymbol{R}^\top > \boldsymbol{0}$, pair ($\boldsymbol{A}, \boldsymbol{Q}$) is detectable) as given by formula (4.12) (Mitkowski, 1991)

$$\boldsymbol{U}^* = \left[F^*_{MR,f}, F^*_{MR,r}, w^*_f, w^*_r \right]^\top = -\boldsymbol{K}\boldsymbol{X} \qquad (4.12)$$

where $\boldsymbol{K}$ is the feedback matrix calculated according to the LQ control law.

In the second stage, the values of control currents i_f, i_r are established such that for instantaneous relative velocities $(\dot{x}_f - \dot{w}_f)$, $(\dot{x}_r - \dot{w}_r)$, the MRAs produce resistance forces $F_{MR,f}$, $F_{MR,r}$ equal to $F^*_{MR,f}$, $F^*_{MR,r}$ (if possible), or of the same sign as $F^*_{MR,f}$, $F^*_{MR,r}$ (if values $F^*_{MR,f}$, $F^*_{MR,r}$ are impossible to produce for the instantaneous relative velocities of the beam and shakers), or equal to zero (if signs of $F^*_{MR,f}$, $F^*_{MR,r}$ are impossible to be produced). This task utilises the hysteresis inverse model (HRM) of the MRA. On the basis of instantaneous values of the signals $\dot{x}$, $\ddot{x}$, $\dot{\varphi}$, $\ddot{\varphi}$, $\dot{w}_f$, $\dot{w}_r$, $\ddot{w}_f$, $\ddot{w}_r$ and the MRA parameters α, β, γ, A, c_0, c_1, k_0, k_1, x_0 at the given operating point (Table 1 and Table 2), the control currents i_f, i_r are determined (Sapiński, 2004). Underlying the design of a nonlinear HRM is the velocity-force relationship for various current levels (Sapiński, 2004).

Figure 8 presents a MATLAB/Simulink diagram of the developed HRM determining the control current of the front MRA. The main blocks of this diagram are:

- *Multi-port switch: HYSTERESIS* modelling the hysteresis of the MRA; its output depends on $(\dot{x}_f - \dot{w}_f)$ and $(\ddot{x}_f - \ddot{w}_f)$

- *Look-up table*: $F_f * /(x'_f - w'_f)$ block for conversion of the quotient: $F^*_{MR,f}/(\dot{x}_f - \dot{w}_f)$ into the current i_f.

The currents i_f and i_r calculated in the described above manner are the output of the cascade controller.

For the given parameters of the experimental setup described in Table 3, the elements of the feedback matrix are as folows

$$\boldsymbol{K} = \begin{bmatrix} -41064 & 3615 & 29213 & 1001 \\ -41072 & 3615 & 29242 & -1000 \\ 0 & 0 & 0 & 0 \\ 0 & 0 & 0 & 0 \end{bmatrix}$$

Zero values of terms in the third and fourth row of the matrix $\boldsymbol{K}$ indicate that no controller action is required to regulate the excitations w_f and w_r such that the optimal value of the quality index is achieved.
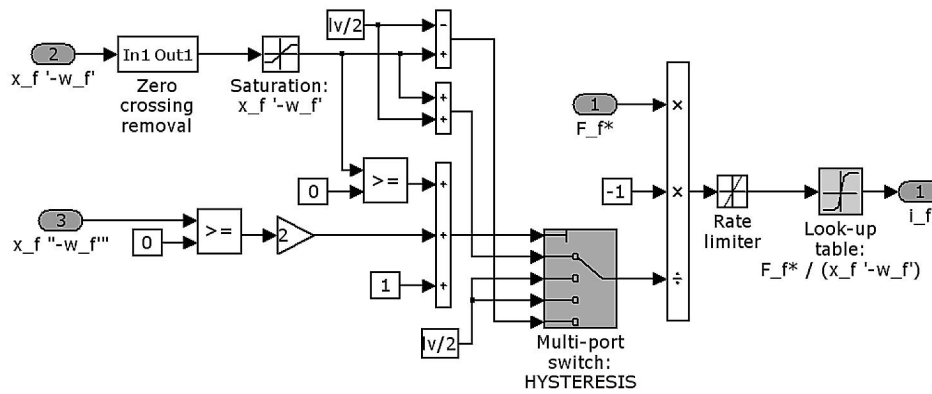
Fig. 8. Simulink diagram of the hysteresis inverse model

Three variants of the cascade controller were studied: HRM-d, in which signals from transducers (x_f, x_r, w_f, w_r) are passed directly to the controller (only a primary low-pass filter is used); HRM with a 1st order inertial filter (time-constant $2 \cdot 10^{-3}$ s) applied to x_f, x_r, w_f, w_r, and HRM-a with the same inertial filter (as HRM) and with additional information on the hysteresis width forwarded to the inverse model.
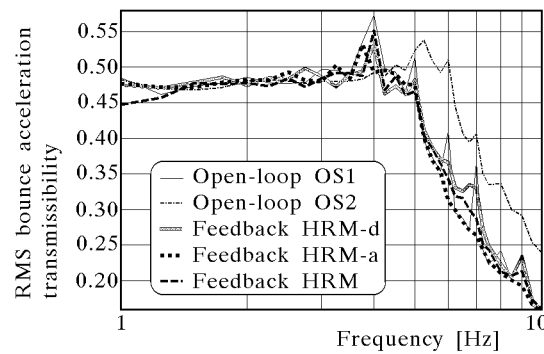

Fig. 9. RMS bounce acceleration transmissibility

Sine excitations in the range of (1,10) Hz were applied to the front suspension-set as it was done for the open-loop system. The effectiveness of the control algorithm described above was evaluated by performing analysis of the c.o.g. RMS bounce and pitch acceleration transmissibilities $T_{\ddot{x}}$ and $T_{\ddot{\varphi}}$ (see Fig. 9 and Fig. 10). Also, the frequency weighted index T_W was evaluated (see Table 4).
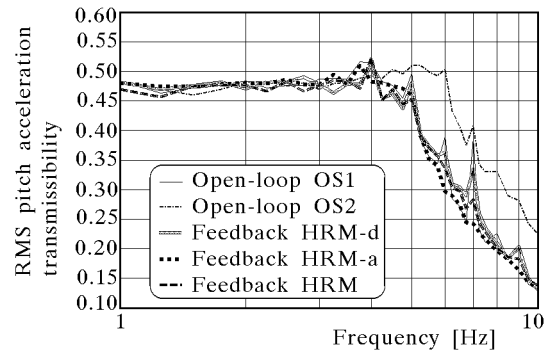
Fig. 10. RMS pitch acceleration transmissibility

Table 4. RMS Acceleration transmissibility

Type of excitation w_f		Open-loop system		Feedback system – cascade controller		
		OS1 $i_f = i_r = 0\text{A}$	OS2 $i_f = i_r = 0.1\text{A}$	HRM	HRM-a	HRM-d
Square (experim.)	$T_{\ddot{x}}$	0.1147	0.2214	0.1161	0.1039	0.1214
	$T_{\ddot{\varphi}}$	0.1373	0.2587	0.1376	0.1254	0.1394
Sine (experim.)	T_W	$2.0066 \cdot 10^3$	$2.2612 \cdot 10^3$	$1.9482 \cdot 10^3$	$1.9306 \cdot 10^3$	$1.9855 \cdot 10^3$
Sine (simulat.)	T_W	$2.3072 \cdot 10^3$	$2.2176 \cdot 10^3$	$2.0858 \cdot 10^3$	$2.1046 \cdot 10^3$	–

Time patterns of the acceleration $\ddot{x}$, displacement x_f and current i_f for the front sine excitation w_f of the frequency of 6 Hz for OS1 (open-loop) and HRM (feedback) systems are shown in Fig. 11. Time patterns of $\ddot{x}$, x_f, i_f, w_f for OS1 and HRM-d systems near the first resonance frequency (at 3.25 Hz) are shown in the Fig. 12.
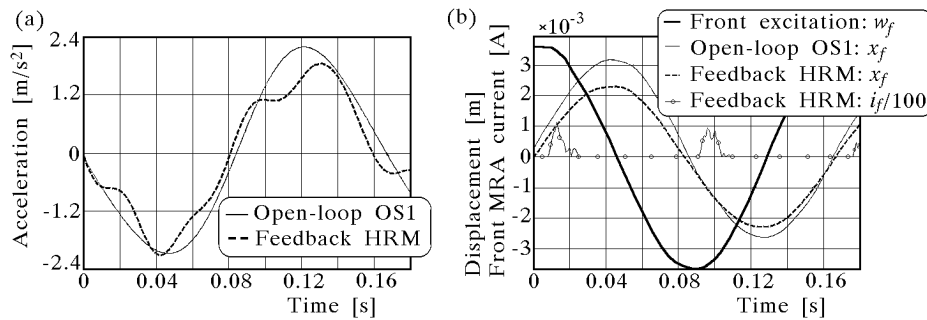

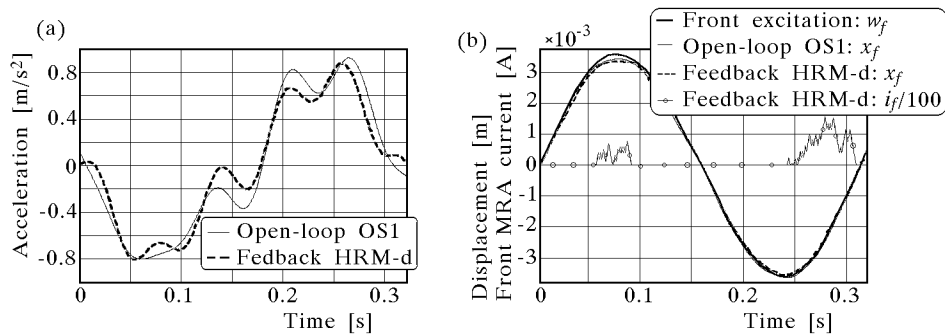Fig. 11. Response to w_f sine excitation at 6 Hz

Fig. 12. Response to w_f sine excitation at 3.25 Hz

Figure 13 presents time patterns of x_f and i_f for the front square excitation of OS1 and HRM-a systems. Respective values of transmissibilities $T_{\ddot{x}}$ and $T_{\ddot{\varphi}}$ are presented in Table 4.
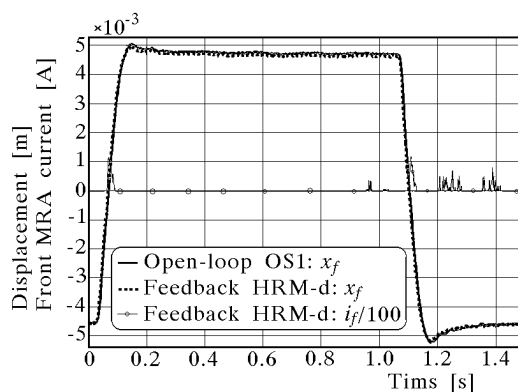

Fig. 13. Response to w_f square excitation

To compare the experimental and simulation results we present, obtained theoretically, bounce and pitch acceleration transmissibilities (Fig. 14 and Fig. 15) and the frequency weighted transmissibility index T_W (Table 4).

5. Discussion of results

The results of experiments evidence advantages of the feedback semi-active suspension system with a cascade controller presented in Section 4.2 over passive (open-loop) systems OS1, OS2. As we observe in Fig. 9 and Fig. 10, the
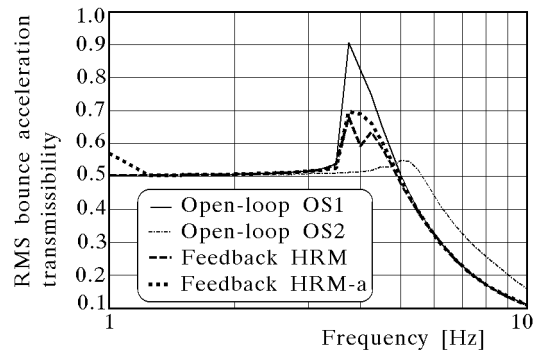
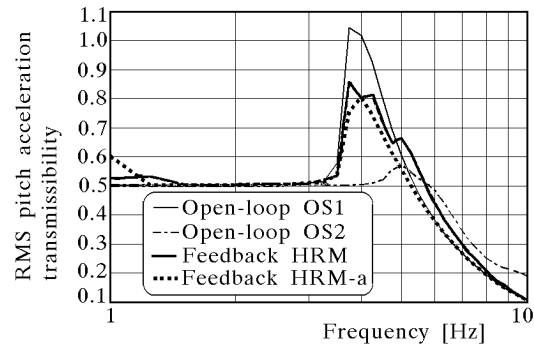Fig. 14. RMS bounce acceleration transmissibility (obtained theoretically)

Fig. 15. RMS pitch acceleration transmissibility (obtained theoretically)

RMS acceleration frequency transmissibilities of systems HRM, HRM-a both lie below the respective characteristics of OS1 and OS2 in most of the frequency ranges. HRM, HRM-d and especially HRM-a systems are characterised with lowered acceleration peaks with respect to OS1, and lowered accelerations at higher frequencies in comparison with OS2. Figure 11a presents reduction of the acceleration $\ddot{x}$ due to controller operation for the 6 Hz front sine excitation. Figure 11b shows the reduction of the displacement x_f due to controller operation, and also the way in which this result is accomplished: the MRA is stiffened (due to current i_f) when the time changes of x_f and w_f are opposite – this implies the reduction of x_f and $\ddot{x}$ amplitudes. Therefore, the controller action is based on the phase difference between x_f and w_f; a significant phase difference guarantees that the amplitude of x_f is smaller than the amplitude of w_f. Figures 12a,b show that the reduction of x_f and $\ddot{x}$, and also the controller action at 3.25 Hz, are not so evident as at 6 Hz (see Fig. 9). Controller operation at 3.25 Hz (Fig. 12b) is visible in the time ran-

ge of $(0.06, 0.09)$ s and also $(0.24, 0.31)$ s. The first action is due to very small phase difference between x_f and w_f, thus very small time range of the opposite changes of x_f and w_f. The second action cause the MRA stiffening to guarantee that the amplitude of x_f is not larger than w_f near the resonance (too small phase difference between x_f and w_f to enable further reduction of x_f amplitude). The time pattern of current i_f for the square excitation also shows the correctness of controller (HRM-a) operation. At the first stage of the response, during and just after the step change of the input, the MRA is soft – this guarantees reduction of the initial shock. After that, when the input is constant, the MRA is rigid (peak of i_f current) to accomplish reduction of over-steer.

One can observe that in the lower frequency range of $(1, 5)$ Hz (including reesonance peaks), the HRM-d controller proves to be the most effective due to the smaller time lag caused by the input filters. However, at higher frequencies, HRM-d does not confirm its advantage over OS1 – the signal filtering seems insufficient and the controller is too sensitive to environmental disturbances, especially during signal differentiation necessary for the MRA inverse model.

The above considerations are borne out by values of the frequency weighted bounce acceleration transmissibility index T_W derived on the basis of the ISO 2631-1 (1997) standard.

Theoretical values of RMS bounce and pitch acceleration transmissibilities of OS1, OS2, HRM and HRM-a systems (Fig. 14 and Fig. 15) and relevant T_W indexes (Table 4) confirm the advantage of the feedback system as well.

6. Conclusions

The paper deals with the experimental study of vibration control in a pitch-plane suspension model equipped with MRAs. Experimental results prove the necessity of implementation and the efficiency of MRAs in vibro-isolation of the investigated suspension system. As the feedback system with additional information on the hysteresis width exhibits the best vibro-isolation features in general, more efforts will be undertaken to develop a more accurate inverse model of the MRA.

Further research will be broadened into a 3 DOF pitch-plane model that will take into account also a driver seat whose suspension is equipped with the MRA.

References

1. Ahmed A.K.W., 2002, *Encyclopedia of Vibration, Ground Transportation Systems*, Academic Press

2. Brzózka J., 2004, *Regulatory i ukady automatyki*, Warszawa

3. Fuller C.R., 1996, *Acive Control of Vibration*, Londyn, Academic Press Ltd.

4. ISO 2631-1, 1997, *Mechanical vibration and shock – Evaluation of human exposure to whole-body vibration*, International Organisation for Standardisation

5. Kiduck K., Doyoung J., 1999, Vibration suppression in a MR Fluid Damper Suspension System, *Journal of Intelligent Material Systems and Structures*, **10**, 779-786

6. Kowal J., 1996, *Sterowanie drganiami*, Kraków, Gutenberg

7. LORD CORPORATION, 2003, http://www.lord.com

8. Martynowicz P., 2003, Simulation of a vehicle suspension with magnetorheological dampers, *Kwartalnik AGH, Mechanika*, **22**, 355-361

9. McLellan N.S., 1998, *On the Development of Real-Time Embeded Digital Controller for Heavy Truck Semiactive Suspensions*, Virginia Tech, Master Thesis

10. Mitkowski W., 1991, *Stabilizacja systemów dynamicznych*, Cracow, AGH

11. Nagai M., Onda M., Hasegawa T., Yoshida H., 1996, Semi-active control of vehicle vibration using continuously variable damper, *Third International Conference on Motion and Vibration Control*, Chiba

12. Pare C.A., 1998, *Experimental Evaluation of Semiactive Magneto-Rheological Suspensions for Passenger Vehicles*, Virginia Tech, Master Thesis

13. Sapiński B., Piłat A., Rosół M., 2003, Modelling of a quarter-car semi active suspension with MR damper, *Machine Dynamics Problems*, **27**

14. Sapiński B., 2004, Linear magnetorheological fluid dampers for vibration mitigation: modelling, control and experimental testing, *Rozprawy, Monografie AGH*, **128**

15. Sapiński B., Martynowicz P., 2004, Sterowanie liniowo-kwadratowe drganiami w ukadzie zawieszenia magnetoreologicznego (Linear-quadratic vibration control for MR suspension system), *Czasopismo Techniczne Politechniki Krakowskiej*, **5**, 335-343

16. Simon D.E., 2000, *Experimental Evaluation of Semiactive Magneto-Rheological Primary Suspensions for Heavy Truck Applications*, Virginia Tech, PhD Thesis

17. Song X., 1998, *Design of Adaptive Control Systems with Applications to Magneto-Rheological Dampers*, Virginia Tech, PhD Thesis

18. Spencer B., 1996, Phenomenological model of a magnetorheological damper, *Journal of Engineering Mechanics*

19. THE MATH WORKS, 2003, Real Time Workshop User's Guide

20. VIRGINIA TECH, 2002, http://www.avdl.me.vt.edu

21. Yao G.Z., Yap F.F., Chen G., Li W.H., Yeo S.H., 2002, MR damper and its application for semi-active control of vehicle suspension system, *Technical Note, Mechatronics*, **12**, 963-973

Sterowanie drganiami w płaskim modelu zawieszenia z amortyzatorami magnetoreologicznymi

Streszczenie

W artykule przedstawiono analizę eksperymentalną sterowania drganiami zawieszenia z dwoma niezależnymi amortyzatorami magnetoreologicznymi. Do analizy wykorzystano model zawieszenia w płaszczyźnie przechyłów wzdłużnych, posiadający dwa stopnie swobody (ruch pionowy i przechył wzdłużny). Model ten zbadano w układach otwartym i zamkniętym przy harmonicznych oraz prostokątnych wymuszeniach kinetycznych. Eksperymenty przeprowadzono na wykonanym według własnego projektu stanowisku badawczym przy użyciu środowiska pomiarowo-sterującego MATLAB/Simulink. Wyniki pomiarów potwierdziły skuteczność sterowania drganiami za pomocą amortyzatorów magnetoreologicznych w rozważanym układzie zawieszenia.